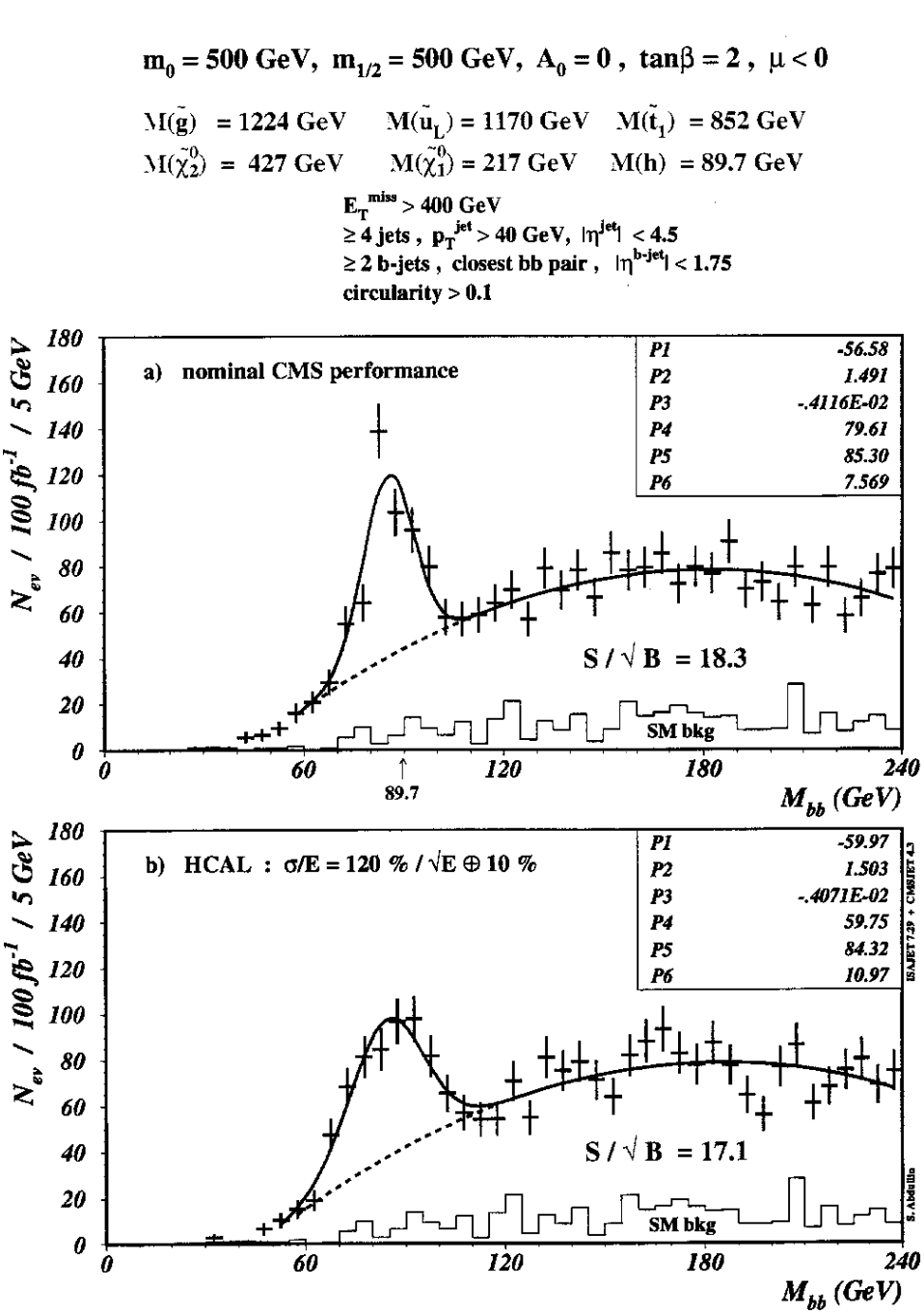
h → bb̄ in mSUGRA
m0 = 500 GeV, m1/2 = 500 GeV, A0 = 0 , tanβ = 2 , μ < 0
M(g̃) = 1224 GeV M(ũL) = 1170 GeV M(t̃1) = 852 GeV
M(χ̃02) = 427 GeV M(χ̃01) = 217 GeV M(h) = 89.7 GeV
ET miss > 400 GeV
≥ 4 jets , pT jet > 40 GeV, |η jet| < 4.5
≥ 2 b-jets , closest bb pair , |η b-jet| < 1.75
circularity > 0.1
a) nominal CMS performance
P1 -56.58
P2 1.491
P3 -.4116E-02
P4 79.61
P5 85.30
P6 7.569
S / √ B = 18.3
SM bkg
89.7
Nev / 100 fb-1 / 5 GeV
Mbb (GeV)
b) HCAL : σ/E = 120 % / √E ⊕ 10 %
P1 -59.97
P2 1.503
P3 -.4071E-02
P4 59.75
P5 84.32
P6 10.97
S / √ B = 17.1
SM bkg
ISAJET 7.29 + CMSJET 4.3
S. Abdullin

Figure 1

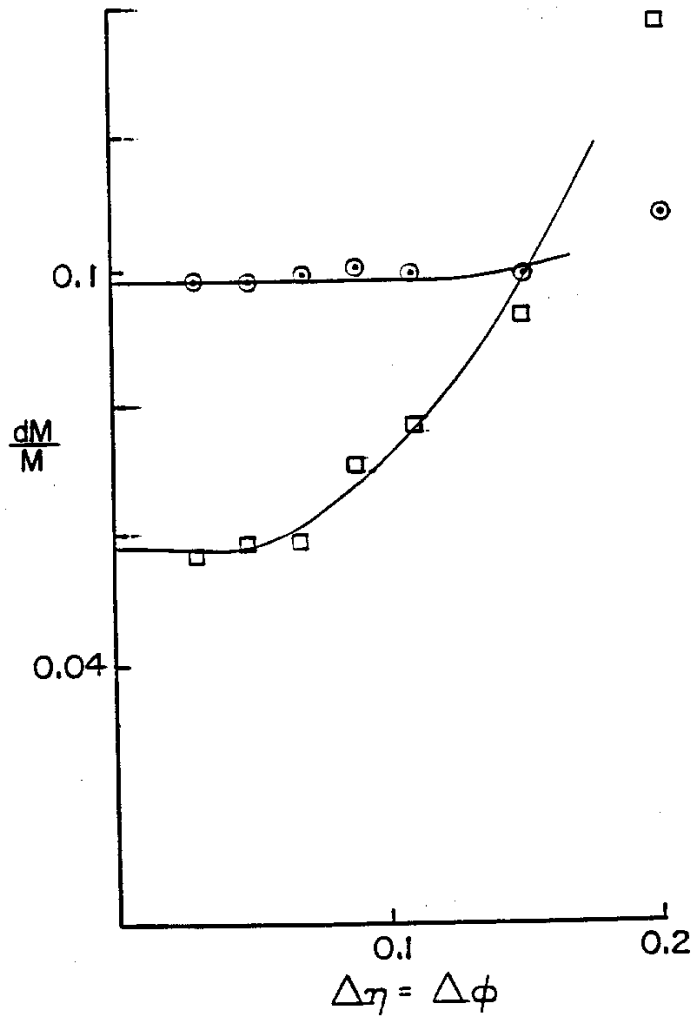

Figure 2

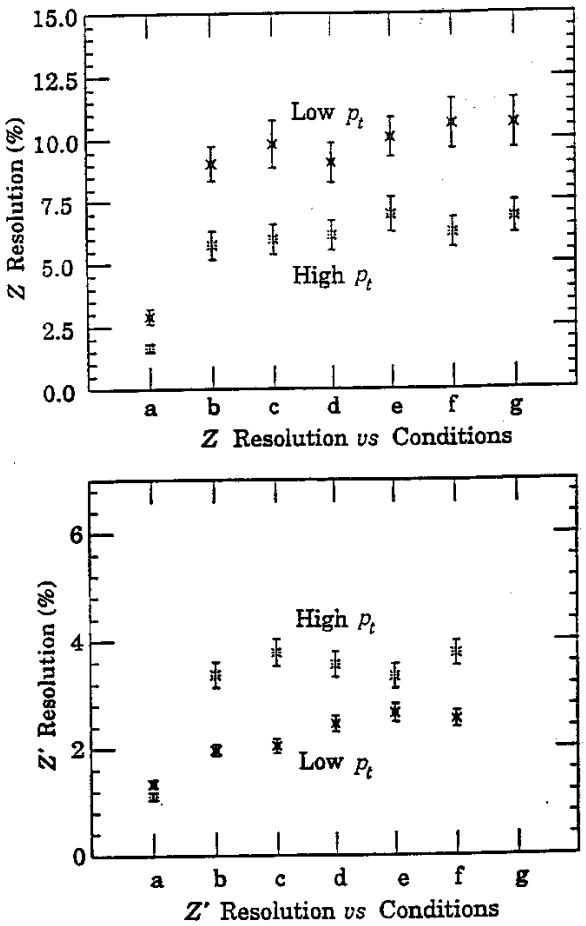
15.0
12.5
10.0
7.5
5.0
2.5
0.0
Z Resolution (%)
Low p_t
High p_t
a
b
c
d
e
f
g
Z Resolution vs Conditions
6
4
2
0
Z' Resolution (%)
High p_t
Low p_t
a
b
c
d
e
f
g
Z' Resolution vs Conditions

Figure 3

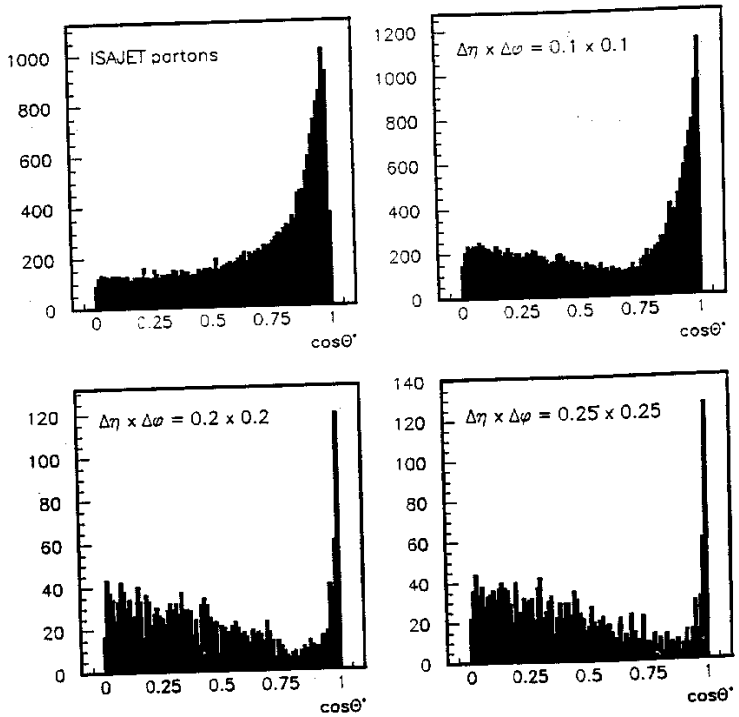

1 Distributions of $\cos\theta^*$ for $W + jets$ background events, with no pileup. The distribution for the ISAJET partons is compared with that found with three different calorimeter segmentations.

Figure 4

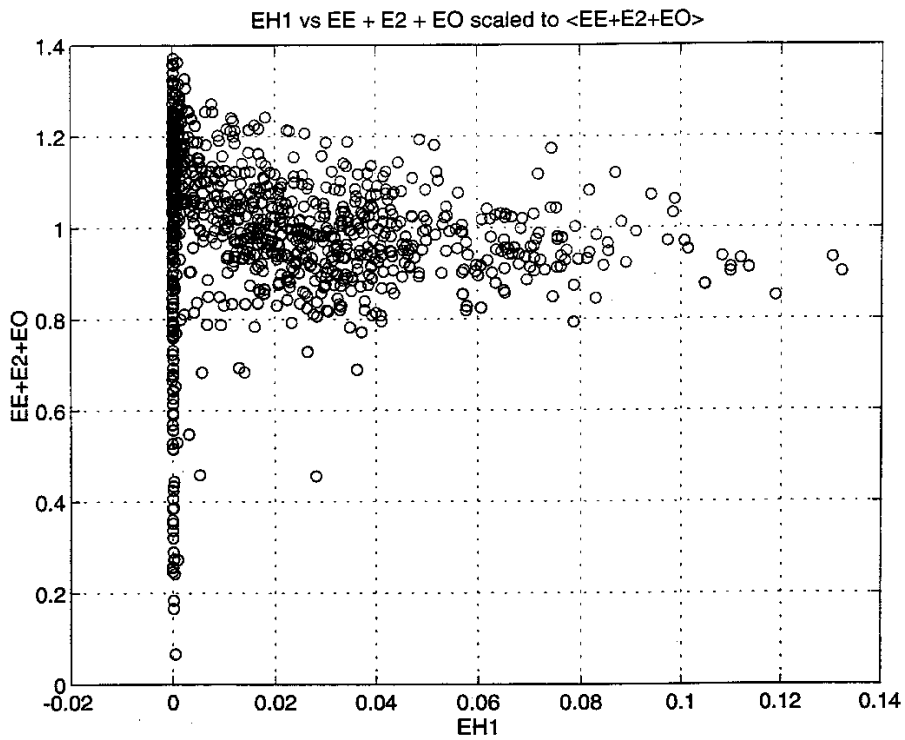
EH1 vs EE + E2 + EO scaled to <EE+E2+EO>
EE+E2+EO
EH1
1.4
1.2
1
0.8
0.6
0.4
0.2
0
-0.02
0
0.02
0.04
0.06
0.08
0.1
0.12
0.14

Figure 5

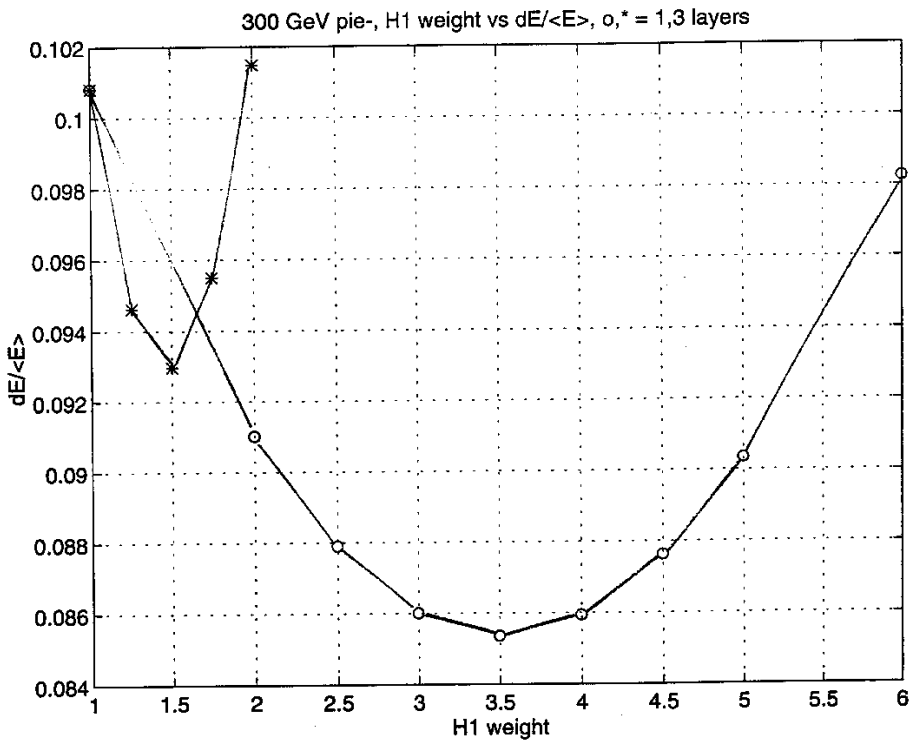
300 GeV pie-, H1 weight vs dE/<E>, o,* = 1,3 layers
0.102
0.1
0.098
0.096
0.094
0.092
0.09
0.088
0.086
0.084
dE/<E>
1
1.5
2
2.5
3
3.5
4
4.5
5
5.5
6
H1 weight

Figure 6 a

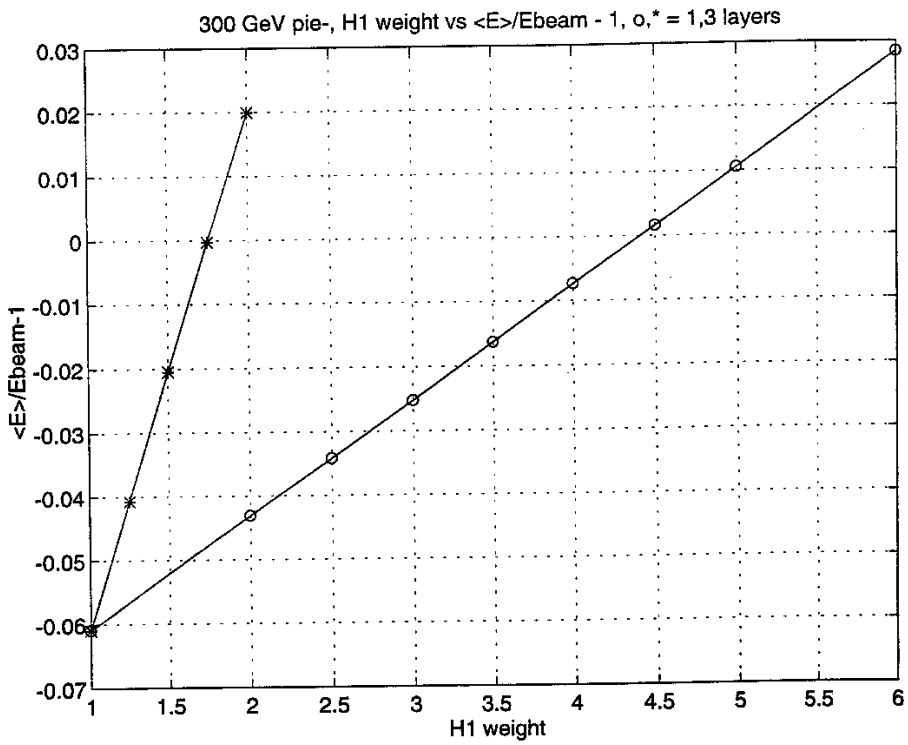
300 GeV pie-, H1 weight vs <E>/Ebeam - 1, o,* = 1,3 layers
0.03
0.02
0.01
0
-0.01
-0.02
-0.03
-0.04
-0.05
-0.06
-0.07
<E>/Ebeam-1
1
1.5
2
2.5
3
3.5
4
4.5
5
5.5
6
H1 weight

Figure 6b

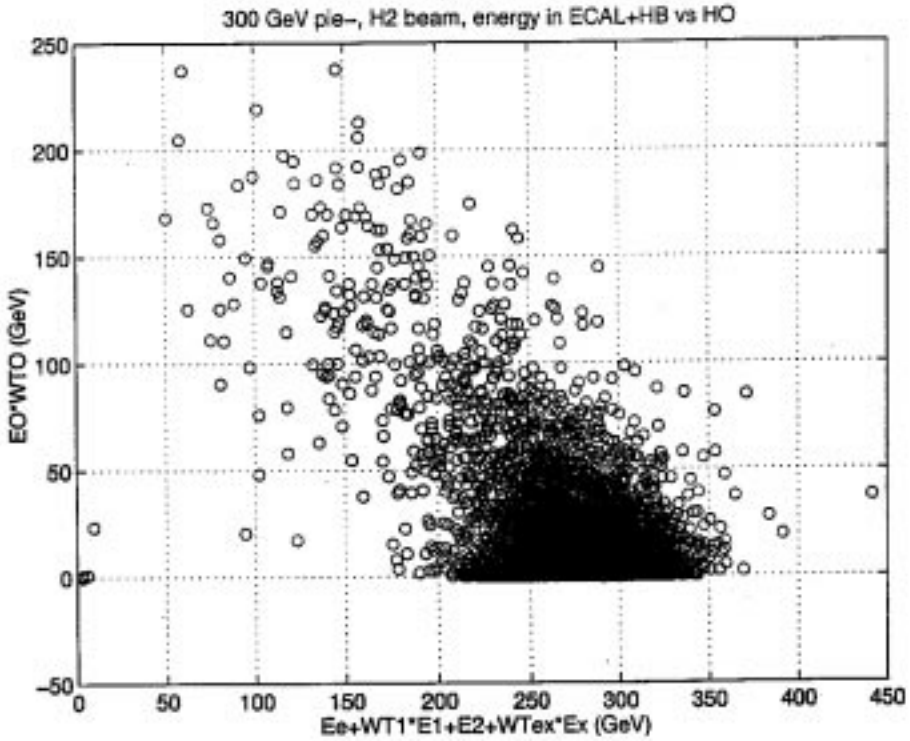
300 GeV pie−, H2 beam, energy in ECAL+HB vs HO
EO*WTO (GeV)
Ee+WT1*E1+E2+WTex*Ex (GeV)
250
200
150
100
50
0
−50
0
50
100
150
200
250
300
350
400
450

Figure 7

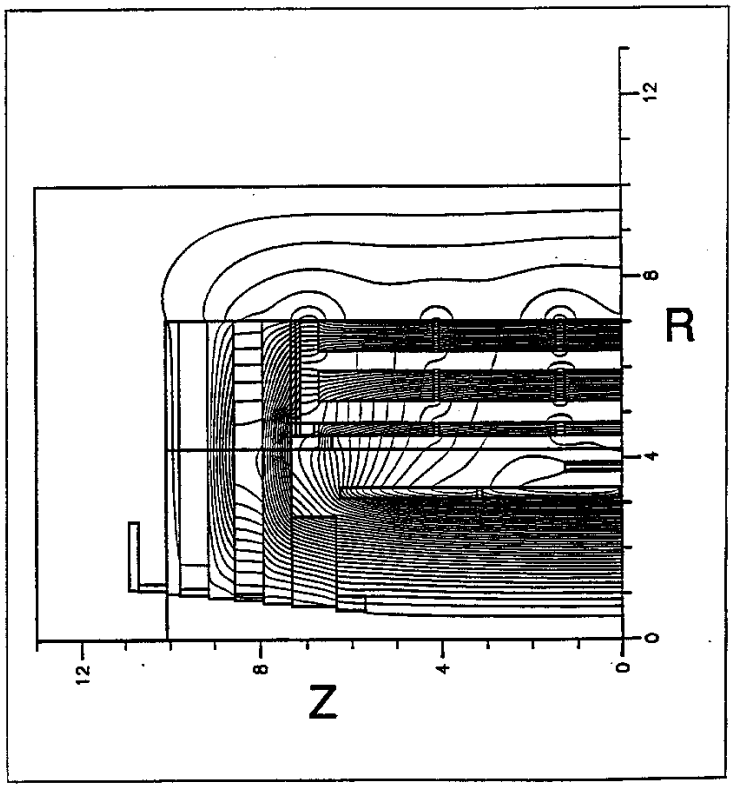

Typical flux line distribution.

Figure 8

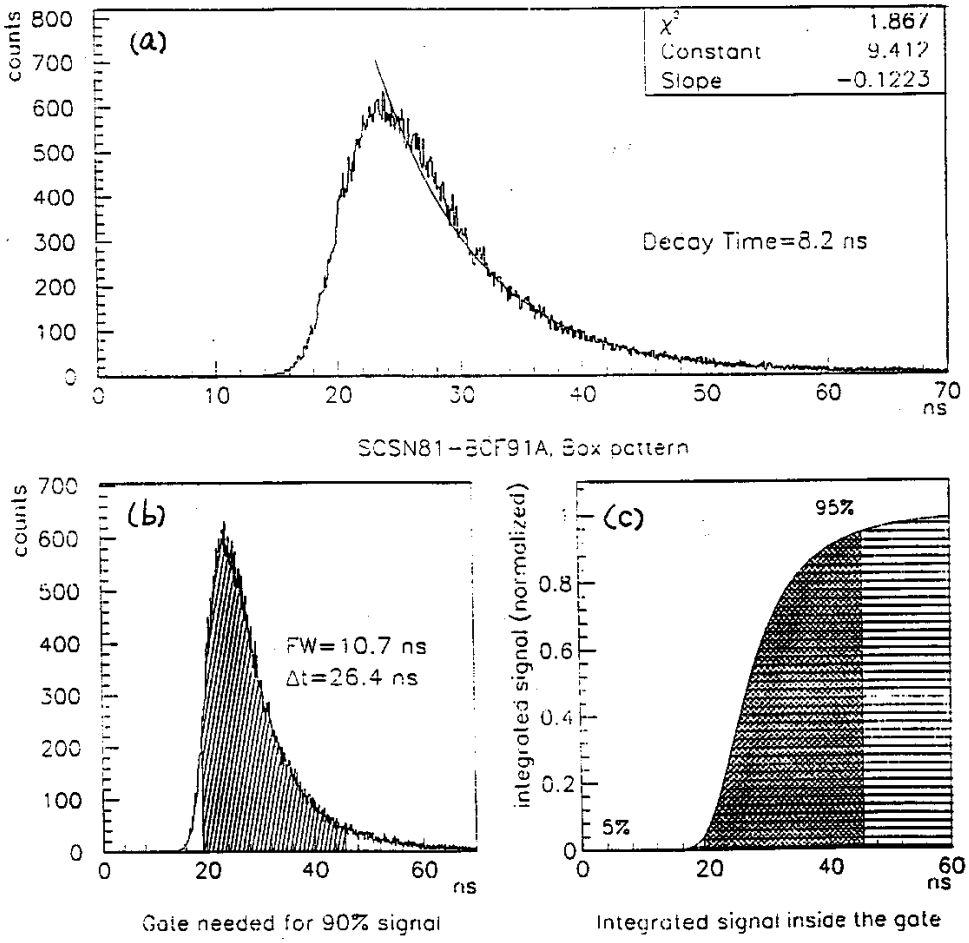

[illegible]: (a) Decay time spectrum of SCSN81/BCF91A, box pattern. Tail of the measured decay spectra was fitted to an exponential function ($= A \cdot e^{-\tau \cdot t}$) to obtain a "decay time ($= \tau$)". (b) The decay spectrum was integrated to obtain the time needed to capture 90% of the signal ($\equiv \Delta t = 90\%$ signal collection time) (c) Integrated signal inside Δt.

Figure 9

PMT Box (Side View)

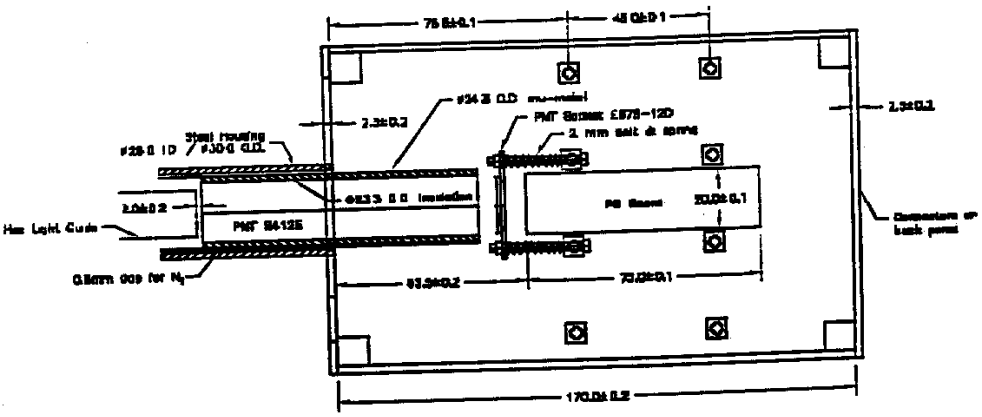

Figure 10

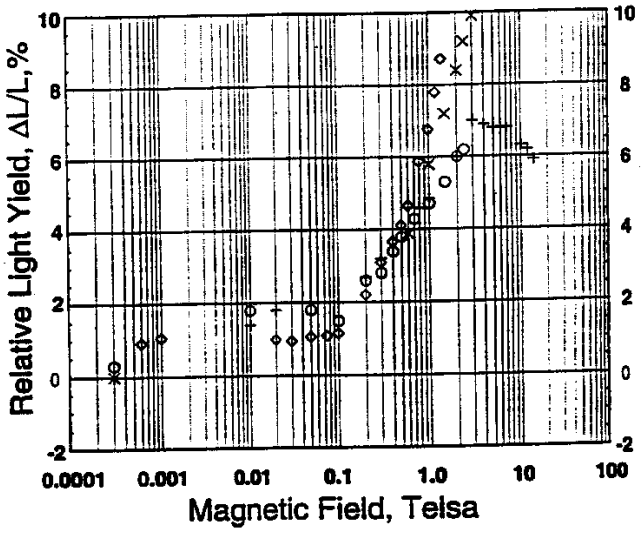

Fig. 11. Relative light yield increase as a function of magnetic field. (o) SCSN38 with ^{226}Ra; (+) SCSN38 with ^{60}Co; (◇) DESY calorimeter with SCSN38 using 6 GeV electrons; (×) Shashlik calorimeter using electron beam.

Figure 11

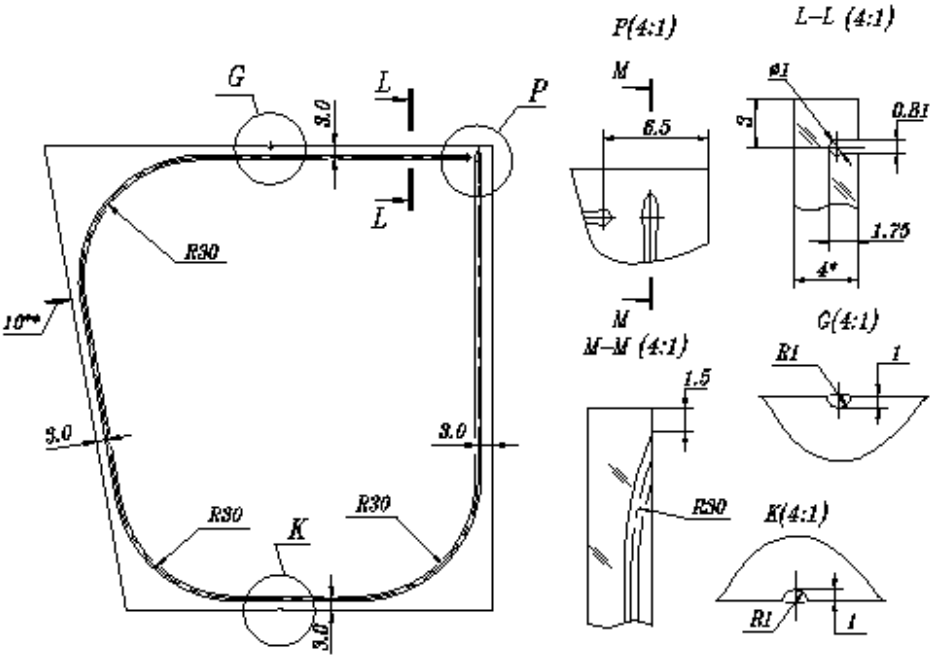
G
L
P
3.0
L
R30
10°
3.0
3.0
R30
K
R30
3.0
P(4:1)
M
6.5
M
M–M (4:1)
1.5
R30
L–L (4:1)
ø1
3
0.81
1.75
4*
G(4:1)
R1
1
K(4:1)
R1
1

Figure 12

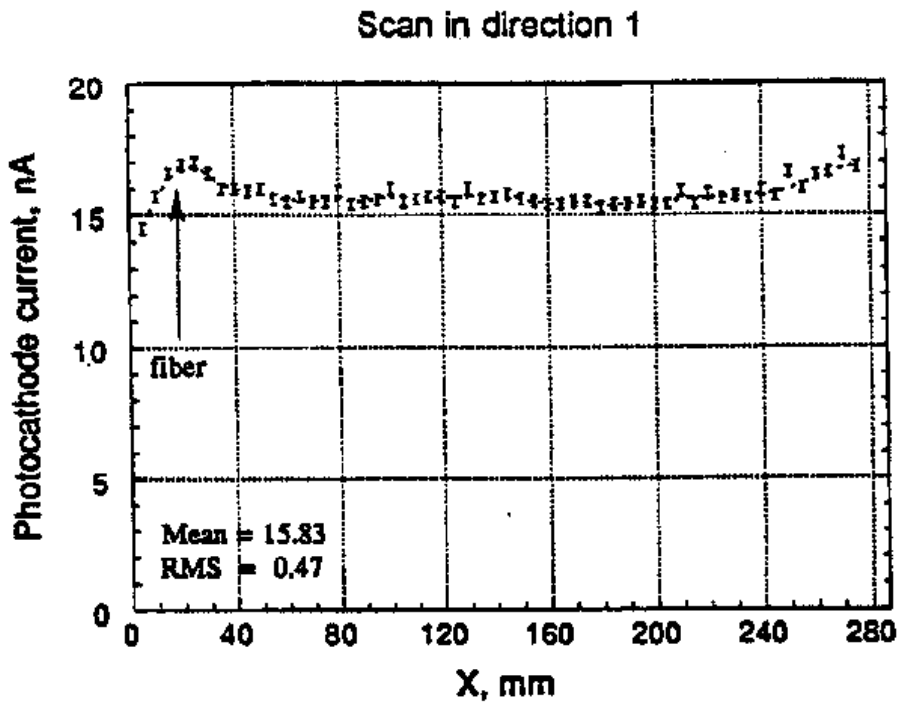
Scan in direction 1
Photocathode current, nA
X, mm
fiber
Mean = 15.83
RMS = 0.47
0
5
10
15
20
0
40
80
120
160
200
240
280

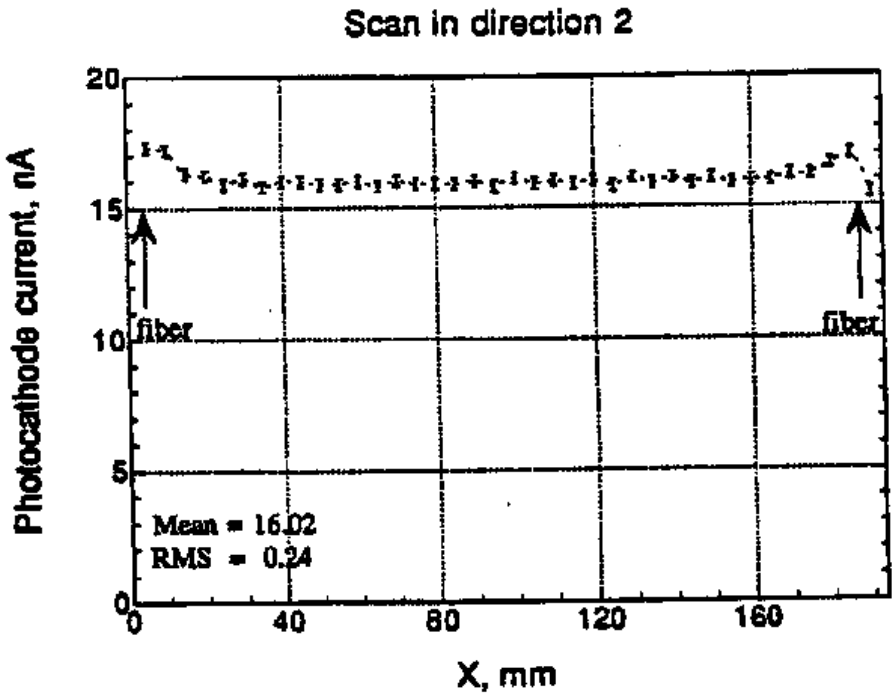
Scan in direction 2
Photocathode current, nA
X, mm
fiber
fiber
Mean = 16.02
RMS = 0.24
0
5
10
15
20
0
40
80
120
160

Figure 13

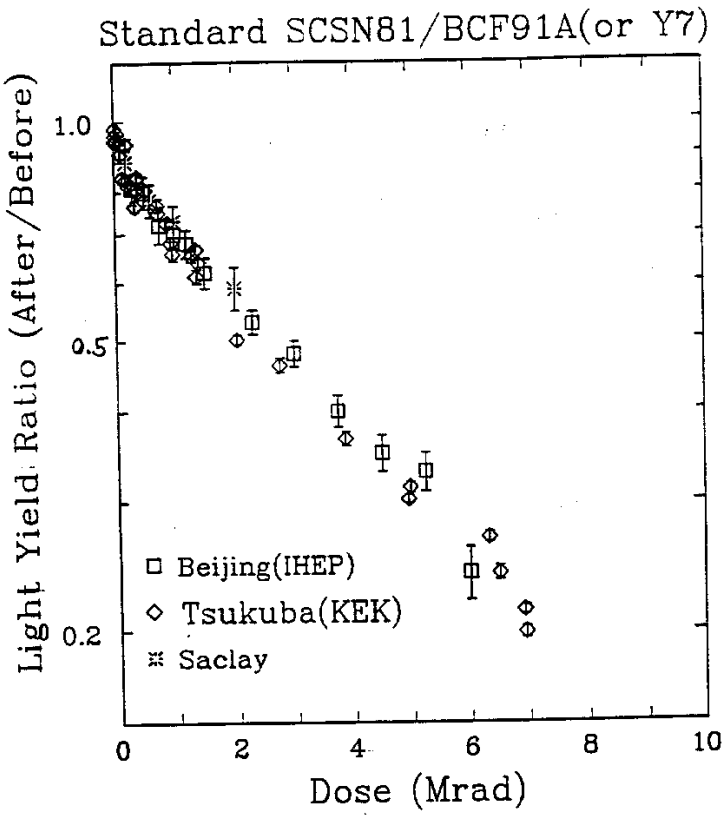

: Radiation hardness (ratio of light yield after to before the irradiation as a function of total dose) for a "standard" tile/fiber - SCSN81/BCF91A(or Y7) measured by beam test modules using electron beam. Data from references [4,5,6].

Figure 14

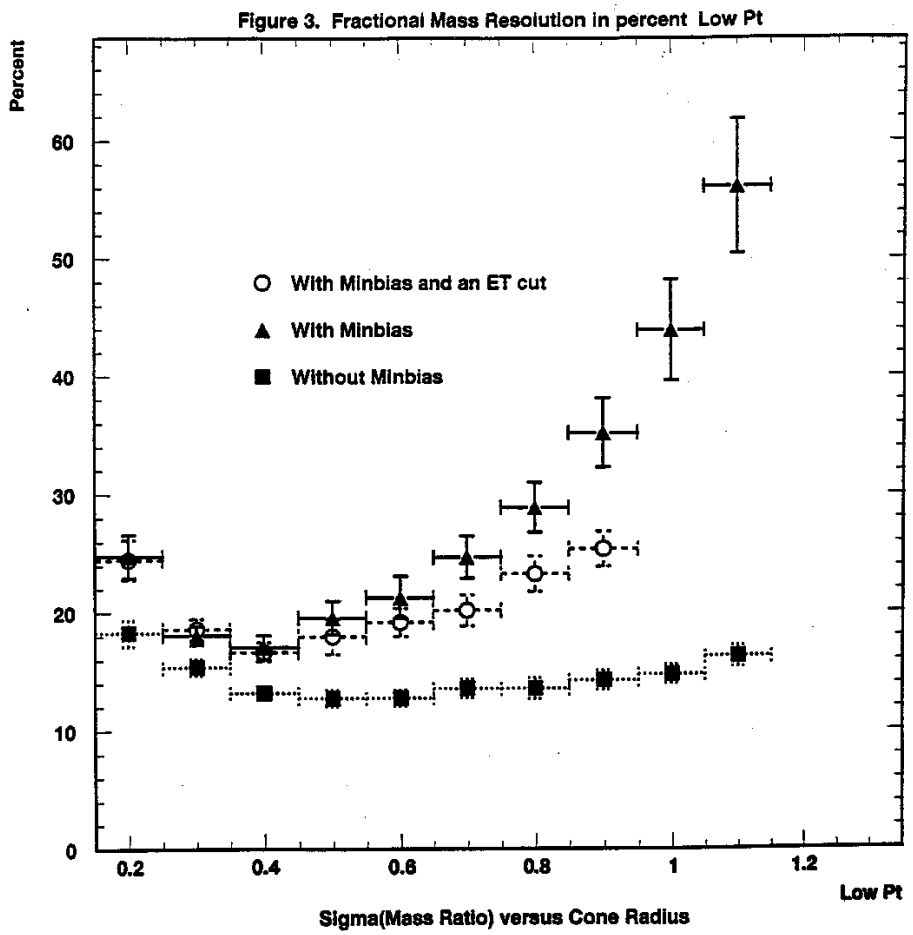
Figure 3. Fractional Mass Resolution in percent Low Pt
Percent
60
50
40
30
20
10
0
0.2
0.4
0.6
0.8
1
1.2
Low Pt
With Minbias and an ET cut
With Minbias
Without Minbias
Sigma(Mass Ratio) versus Cone Radius

Figure 15

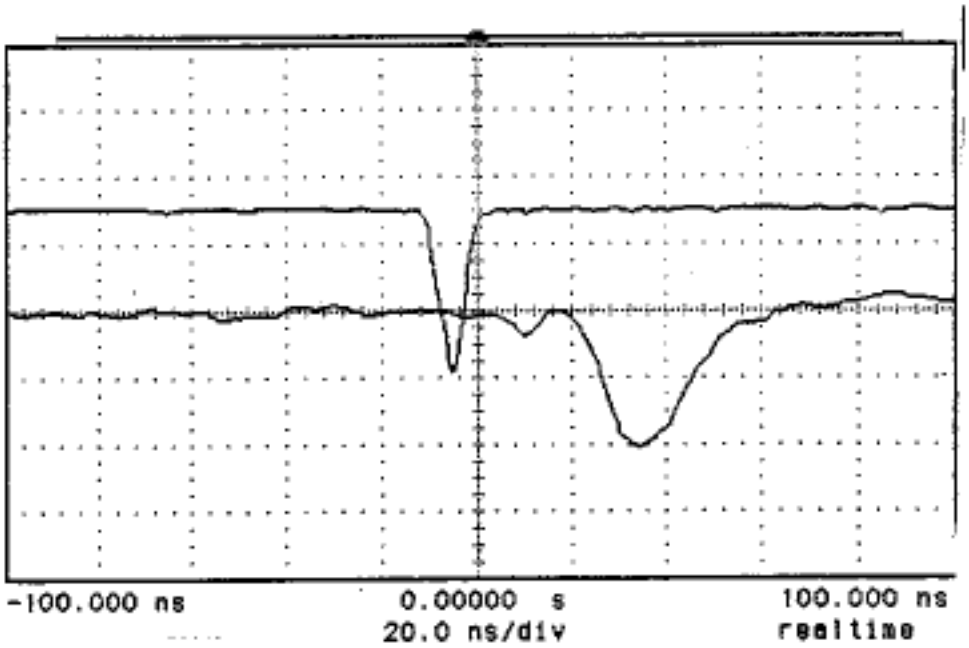
-100.000 ns
0.00000 s
20.0 ns/div
100.000 ns
realtime

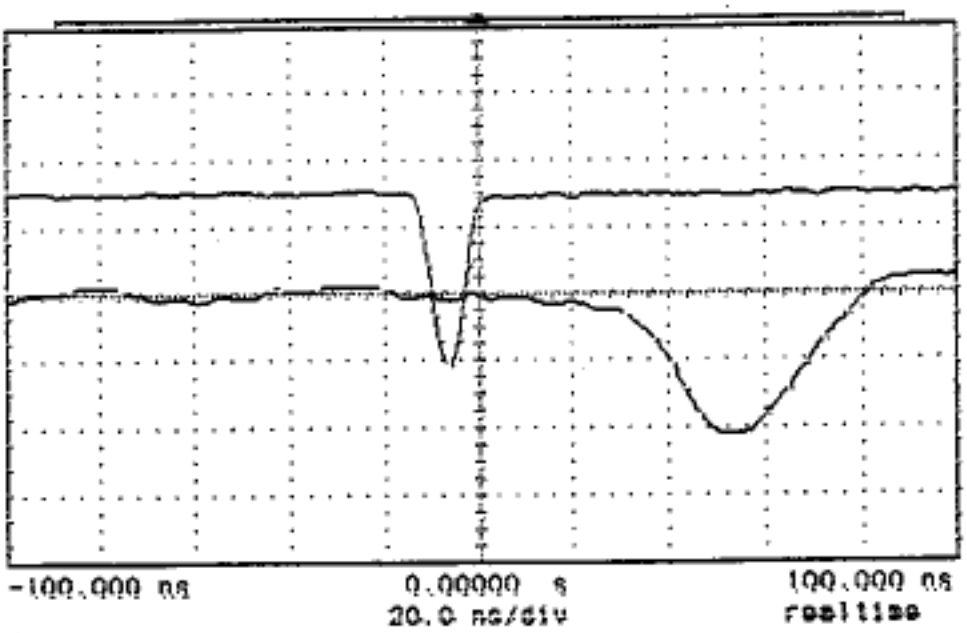
-100.000 ns
0.00000 s
20.0 ns/div
100.000 ns
realtime

Figure 16